Supporting information

Hierarchical Engineering of Mn_2O_3/Carbon Nanostructured Electrodes for Sensitive Screening of Acetylcholine in Biological Sample

M. Y. Emran[a,b], M. A. Shenashen[a,c], A. Elmarakbi[d], M. M. Selim[e], S. A. El-Safty [a,*]

[a] National Institute for Materials Science (NIMS), Research Center for Functional Materials, 1-2-1 Sengen, Tsukuba-shi, Ibaraki-ken 305-0047, Japan.

[b] Chemistry Department, Faculty of Science, Al-Azhar University, Assiut 71524, Egypt

[c] Department of Petrochemical, Egyptian Petroleum Research Institute (EPRI), Cairo 11727, Egypt

[d] Faculty of Engineering and Environment, Northumbria University, Newcastle upon Tyne, NE1 8ST, UK.

[e] Al-Aflaj College of Science and Human Studies, Prince Sattam Bin Abdulaziz University, Al-Aflaj, 710-11912, Saudi Arabia.

*Correspondence: sherif.elsafty@nims.go.jp

Homepage: https://samurai.nims.go.jp/profiles/sherif_elsafty

Experimental section

1.1 Materials

All chemicals were of analytical grade and were used without further purification. Sodium Dopamine hydrochloride, potassium permanganate ($KMnO_4$), adrenaline, noradrenaline, uric acid (UA), tryptophane, guanine, glucose (gl), potassium ferricyanide [$K_3Fe(CN)_6$], human blood serum, and potassium chloride (KCl) were purchased from Sigma-Aldrich Company, Ltd., USA. L(+)-ascorbic acid (AA), adenine, and sodium citrate were purchased from Wako C2.3

1.2 Electrochemical detection of ACh on Mn$_2$O$_3$NLs/C/GCE and Mn$_2$O$_3$FL/C/GCE

The ACh concentrations were detected using a nonenzymatic-based sensor of $Mn_2O_3NLs/C/GCE$ and $Mn_2O_3FL/C/GCE$. The electrochemical measurements were set using three-electrode systems with $Mn_2O_3NLs/C/GCE$, $Mn_2O_3FL/C/GCE$, and GCE as the working electrodes, Ag/AgCl (3 M NaCl) as the reference electrode, and Pt wire as the counter electrode. The supporting electrolyte was 0.1 M NaOH. Various electrochemical techniques, such as CV, electrochemical impedance spectroscopy (EIS), and chronoamperometry (CA), were set and performed using a Zahner/Zennium electrochemical workstation (Thales Z 2.0 software). ompany, Ltd., Osaka, Japan.

1.2 Characterization analyses

The architectonic configurations and geometrics of of Mn_2O_3 materials and electrodes are investigated by using a wide range of advanced techniques such as X-ray diffraction (XRD) using an 18 kW diffractometer (Bruker D8 Advance X-ray diffractometer) ,and field emission-type scanning electron microscope FE-SEM (JEOL JSM-Model 7000F, JEOL Ltd). The various heterogeneous composites and surface topologies and parameters of Mn_2O_3NLs/C and Mn_2O_3FL/C were investigated usingX-ra y photoelectron spectroscopy (XPS) (PHI Quantera SXM (ULVAC-PHI) instrument (Perkin–Elmer Co., USA)), Fourier transform-infrared (FT-IR) and Raman spectroscopy (HR Micro Raman spectrometer, Horiba, Jobin Yvon).The Raman shift spectra were performed at a power of 0.5 eV, laser wavelength $ƛ$= 532 nm, scanning for 10 times, and time exposure of 10 s in range of $450 − 2800$ cm^{-1}.

3. Results and discussions

Electrode surface area

The $Mn_2O_3NLs/C/GCE$, $Mn_2O_3FL/C/GCE$, and GCE surface areas were explored based on the Rundles–Sevick equation [1]:

$$I_p(A) = 2.69 \times 10^5 \ n^{3/2} \ A_0 D_0^{1/2} C_0 v^{1/2}$$

Where, I_p is the anodic current value (A), n denotes the electron transfer, D represents the diffusion coefficient (cm^2 s^{-1}), C_o refers to the [$K_3Fe(CN)_6$] concentration (mol cm^{-3}), v is the scan rate value (Vs^{-1}), and A is the electrode surface area (cm^2).
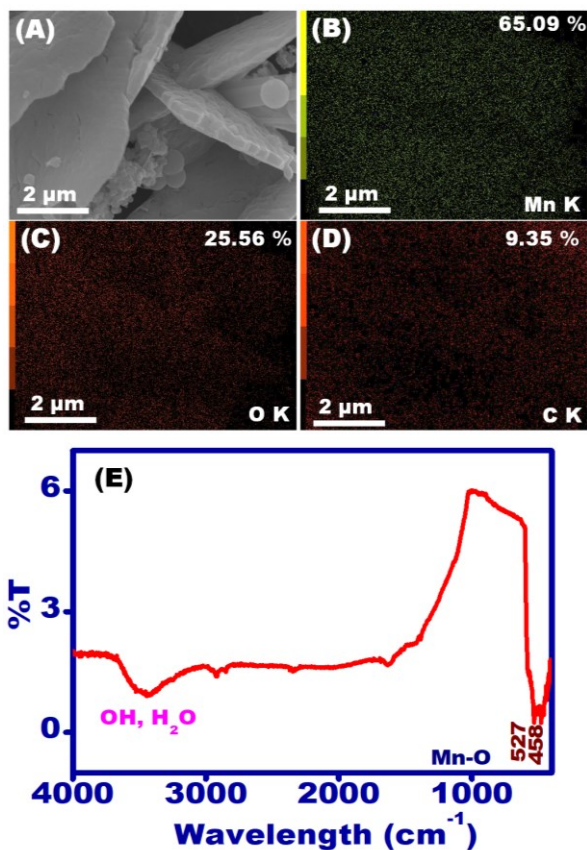
Figures

Figure S1. A) The EDX-SEM mapping of Mn (B), O (C), and C (D). E) the FT-IR of Mn_2O_3/C.
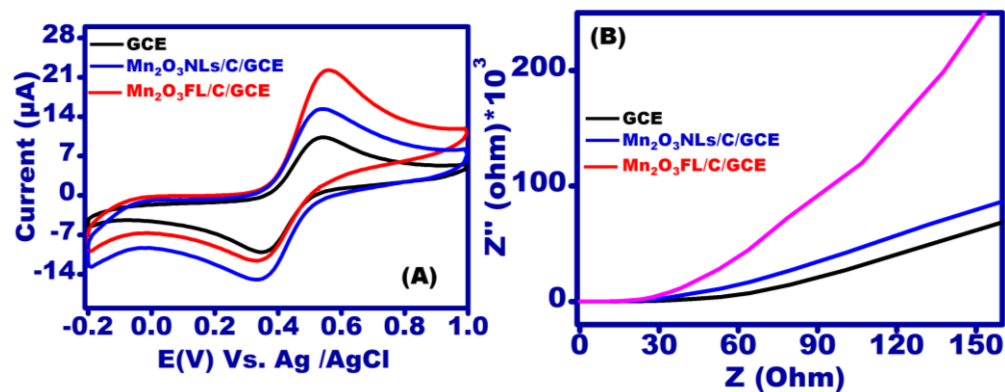
Figure S2. The CVs (A) and impedence spectroscopy (-Nyquest plot) (B) of GCE (black line), Mn_2O_3NLs/C/GCE (blue line), and Mn_2O_3FL/C/GCE (Red line) in 0.1 M KCl containing 1 mM $[Fe(CN)_6]^{3-/4-}$ at scan rate of 100 mVs^{-1}.
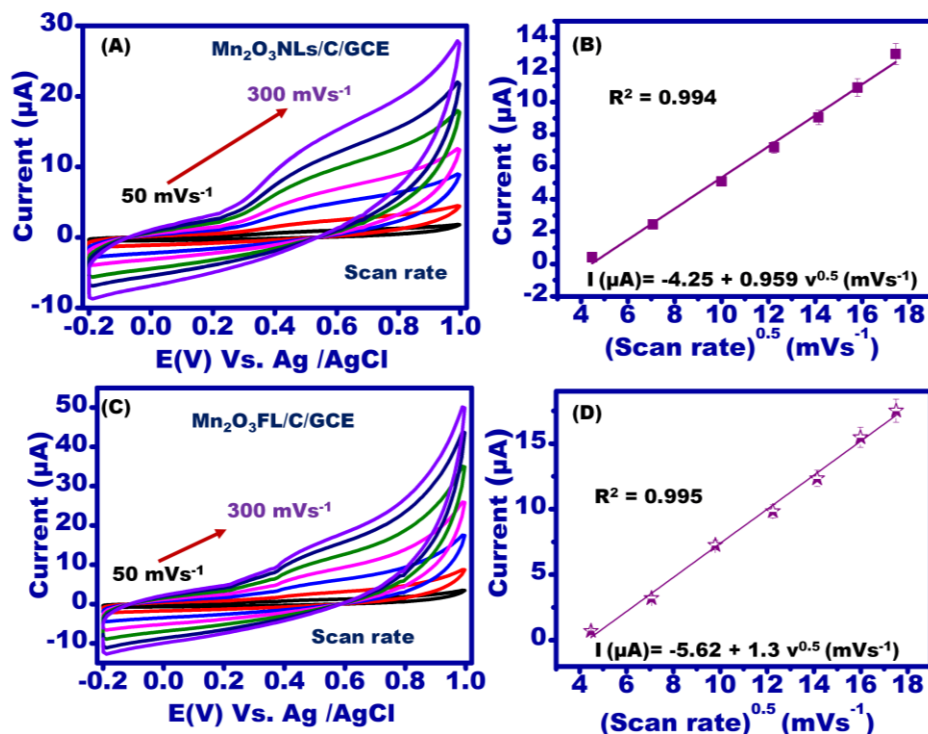
Figure S3. The CVs of 1.5 mM ACh in 0.1 M NaOH at various scan rates of 50 –300 mVs^{-1} using Mn$_2$O$_3$NLs/Cs/GCE (A) and Mn$_2$O$_3$FL/C/GCE. B) The plot of square root of scan rate (mVs^{-1}) versus the relevant current (µA) for Mn$_2$O$_3$NLs/C/GCE (C) and Mn$_2$O$_3$FL/C/GCE (D).

Table S1. The comparison of various electrode design materials and the designed materials of Mn$_2$O$_3$NLs/C and Mn$_2$O$_3$FL/C on the bases of linear range and limit of detection (LOD) (µM) .

Electrode materials	Linear range (µM)	LOD (µM)	Ref
Ni−Al LDHs/OMC/GC	2−4922	0.042	2
NiAl-LDH/CD composites	5 – 6885	1.7	3
hollow nickel microspheres/ carbon	0.24 –828	0.049	4
copper nanoparticles	120–2680	39	5
Cu@Cu2O-BNDC	0.3 –2602	17	6
nickel oxide nanostructure	250 –5880	26.7	7
CuCo2O4 nanoplates	0.2 – 3500	0.03	8
MCSNP/SPE	0.1–500	0.02	9
Mn$_2$O$_3$NLs/C	100 – 7000	7	Current
Mn$_2$O$_3$FL/C	100 – 6500	2	work

References

1. D. Buttry and A. Bard, *Electroanalytical chemistry*, 1991, **17**.

2. J. Ju, J. Bai, X. Bo, L. Guo, *Electrochim. acta*, 2012, **78**, 569-575.

3. L. Wang, X. Chen, C. Liu, W. Yang, *Sens. Actuators B: Chem.*, 2016, **233**, 199-205.

4. N. Sattarahmady, H. Heli, A. Moosavi-Movahedi, *Biosens. Bioelectron.*, 2010, **25**, 2329-2335.

5. H. Heli, M. Hajjizadeh, A. Jabbari, A.A. Moosavi-Movahedi, *Biosens. Bioelectron.*, 2009, **24**, 2328-2333.

6. P. Balasubramanian, T. Balamurugan, S.-M. Chen, T.-W. Chen, T. Sathesh, *ACS Sust. Chem. Eng.,* 2018, **7**, 5669-5680.

7. N. Sattarahmady, H. Heli, R.D. Vais, Biosens. Bioelectron., 2013, **48**, 197-202.

8. P. Balasubramanian, T.S.T. Balamurugan, S.-M. Chen, T.-W. Chen, ACS Sust. Chem. Eng., 2019, **7**, 7642-7651.

9. S.Z. Mohammadi, H. Beitollahi, S. Tajik, *Micro & Nano Syst. Lett.,* 2018, **6**, 1-7.